

# ECI: a Customizable Cache Coherency Stack for Hybrid FPGA-CPU Architectures

Abishek Ramdas

Systems Group, D-INFK, ETH Zurich  
Zurich, Switzerland

Michael Giardino

Systems Group, D-INFK, ETH Zurich  
Zurich, Switzerland

Runbin Shi

Systems Group, D-INFK, ETH Zurich  
Zurich, Switzerland

Adam Turowski

Systems Group, D-INFK, ETH Zurich  
Zurich, Switzerland

David Cock

Systems Group, D-INFK, ETH Zurich  
Zurich, Switzerland

Gustavo Alonso

Systems Group, D-INFK, ETH Zurich  
Zurich, Switzerland

Timothy Roscoe

Systems Group, D-INFK, ETH Zurich  
Zurich, Switzerland

## ABSTRACT

Unlike other accelerators, FPGAs are capable of supporting cache coherency, thereby turning them into a more powerful architectural option than just a peripheral accelerator. However, most existing deployments of FPGAs are either non-cache coherent or support only an asymmetric design where cache coherency is controlled from the CPU. Taking advantage of a recently released two socket CPU-FPGA architecture, in this paper we describe A Customizable Caching Interface (ACCI), a flexible implementation of cache coherency on the FPGA capable of supporting both symmetric and asymmetric protocols. ACCI is open and customizable, given applications the opportunity to fully interact with the cache coherency protocol, thereby opening up many interesting system design and research opportunities not available in existing designs. Through extensive microbenchmarks we show that ACCI exhibits highly competitive performance and discuss in detail one use-case illustrating the benefits of having an open cache coherency stack on the FPGA.

## 1 INTRODUCTION

The multicore era sparked debate about whether alternatives to coherence were required as core count increased [11, 28], or whether cache coherence could simply continue to scale [31]. Its impact on performance [21] is as yet unresolved. Yet, with the proliferation of accelerators such as FPGAs, the question is as relevant today as it was then, and remains open both in terms of its impact on functionality and performance as well as in which protocol is most suitable in which context.

Based on experience with multicore systems one might intuitively assume that cache coherence is always a good feature to have, but on close examination coherence across heterogeneous components is a difficult and complex topic with many implications for performance and ease of use [34]. The “right” solution at this point is far from obvious, and the benefits of coherence in different systems, workloads, and use-cases are poorly understood and not yet sufficiently explored to make any data-backed claims.

This paper takes a fresh perspective on coherence in a heterogeneous system. Rather than asking whether coherence is the right or wrong approach, we step back and pose a different question: what

advantages can different *parts* of a representative coherence protocol *implementation* offer heterogeneous accelerators in a system? We argue the heterogeneity and flexibility provided by accelerators, especially FPGAs, is too large for a single approach to coherence to make sense across all use cases, an argument that has also been made for, e.g., GPUs [34]. In addition, in FPGAs one must be careful with the physical space needed to support cache coherency, which often involves complex protocols with hundreds of states.

There are several ongoing efforts to standardize connections between accelerators and CPUs (e.g., Gen-Z [17], CCIX [9], CXL [15]). These are closed systems in the sense that they provide a single model of coherency with few ways to explore options, alternative designs, or opportunities to tailor the protocol to particular applications. Moreover, they impose an additional protocol translation between CPU and accelerator, rather than talking directly to the CPU’s cache controller. Most importantly, however, these standards conflate separate concerns: cache coherence, caching itself, and communication with the accelerator. Entangling these aspects necessarily leads to compromises in the design, and consequent inefficiencies, not to mention lost opportunities for more direct interaction. Moreover, they make the protocol more complex, increasing the difficulty of efficiently implementing it on an FPGA. A key insight in this paper is that, by separating these three concerns, it is possible to implement an efficient and effective cache coherency stack on the FPGA that allows it to fully interact with the CPU as an equal.

Based on this insight, we have developed an *open cache coherency protocol* that uses minimal FPGA resources and shows competitive performance. The resulting artifact provides an excellent example of how to customize the cache coherency protocol to particular applications, a feature that will enable researchers and developers to manipulate different aspects of coherency to tailor it to concrete applications. The protocol, A Customizable Caching Interface (ACCI), has been implemented on the recently-released open-source research computer Enzian [12] which has an FPGA (Xilinx XCVU9P) located in one of the two sockets of a server-class heterogeneous computer system (ARM ThunderX-1). ACCI is fully compatible with the CPU’s native, inter-socket coherency implementation and thus provides a realistic and fully-functional cache coherency stack.

In this paper we focus on the design of ACCI, its efficient implementation, and explore a concrete use case that demonstrates the potential of ACCI as a tool to implement coherent heterogeneous CPU-FPGA systems. The use case we explore focuses on offloading near-memory-processing operations of increasing complexity (sequential access plus filtering, pointer chasing, and regular expression filtering) to the FPGA. This effectively turns the FPGA into a smart memory management unit, treating FPGA memory as memory in a different NUMA node and returning results directly into the L2 cache of the requesting core, much as a read or write operation over conventional memory would do. This use case offers a nice contrast to existing work implementing similar functionality in restricted settings such as the garbage collection accelerator implemented as part of a RISC-V processor architecture [30] or ACCORDA, a near-memory accelerator prototyped on an FPGA and intended to be inserted on the path between caches and CPUs to offload SQL data processing [16]. For reasons of space, we leave other, more complex use cases that involve manipulating coherency for future work. The use case we analyze in detail demonstrates the feasibility of having a fully compatible implementation of the CPU cache coherency protocol on the FPGA, how tailoring the protocol to the task simplifies it considerably, and the overall performance advantages of ACCI over the bulk data transfer models commonly used today. The idea that a cache coherency protocol can be used for more than just maintaining coherency is starting to gain attention, in particular in relation to accelerators [6, 8]. ACCI provides an open protocol that boosts such efforts by enabling deeper access to the cache coherency protocol and exploring what cache coherency levels or protocol parts are useful for accelerators.

## 2 BACKGROUND

In this section, we summarize existing CPU coherence protocols [32, 34], examine how coherent accelerators and heterogeneous systems affect coherency protocols, and look at the types of applications often accelerated and how they benefit from different coherency models.

### 2.1 The past and present of coherence

Coherence protocols fall into two classes: *snooping* [40] and *directory-based* [10, 47]. Snooping protocols are implemented in symmetric multiprocessor (SMP) systems where all cores share a bus. They are broadcast protocols: whenever a core requires a cache line, it makes a coherence request on the shared bus which is broadcast to all cores. The remaining cores’ coherence controllers check if they have a copy of this cache line in their cache and take appropriate action to maintain coherence. Snooping protocols suffer from scalability and performance limitations because broadcasting becomes expensive when more coherence controllers are added to the system.

Directory protocols are implemented in coherent NUMA systems. Whenever one of the NUMA nodes requires a cache line, it unicasts a request only to the node that is the “home” for that cache line. The home node contains a directory that stores information on which nodes have a copy of this cache line and in what states. The home node then communicates with just the owner or sharers to ensure coherence. Directory protocols do not require broadcasting

messages and so can scale efficiently but latency can suffer as additional messages need to be sent via the home node. Systems such as AMD’s Coherent HyperTransport and HyperTransport Assist, or Intel’s QPI implement versions of directory protocols [34].

Coherence protocols can also be classified by how they handle writes to a local copy of a cache line [34]: *Write-invalidate* protocols, like MSI, MESI, MOESI and MESIF, ensure a single writer by invalidating the copies of a cache line in all other caches. New coherence requests must be made if another core wants to read the updated copy of the cache line. In a *write-update* protocol, whenever a core wants to write to a cache line, it issues a coherence request to update all copies of this cache line. Although write-update protocols reduce the latency of reading a newly updated cache line, they are difficult to scale because update messages are larger than invalidate messages. As a result write-invalidate protocols are more common.

The most basic protocol, MSI, consists of three stable states *modified*, *shared* and *invalid*. A cache line in modified state indicates the cache has the only copy of the cache line in the system and it can therefore be modified. A shared state means that the cache has a read-only copy. Other copies may exist, but must also be in shared state. The MESI, MOSI, MOESI, and MESIF protocols are optimizations of MSI considering additional states. MESI adds an *exclusive* state to indicate that the cache holds the only copy of the cache line in the system and the copy is clean. MOSI, also called the Berkeley protocol [27], adds an additional *owned* state. MOESI, perhaps the most commonly implemented variant, includes both exclusive and owned states. MESIF [26] was developed by Intel and extends the MESI protocol with a *forward* state.

In practice, race conditions and concurrency mean that real implementations have many hidden, intermediate states which greatly complicate the protocol — it is not unusual for a coherency protocol in a multsocket system to have more than 100 states. As a result, without exception, these protocols all target CPU-based systems where multithreaded software shares a single, coherent virtual address space. If taken as they are, it is likely that an implementation of such protocols on an FPGA would be both inefficient and require too much real state, an argument often made when choosing an asymmetric protocol over a symmetric one (see below) or removing cache coherency completely from the FPGA.

In addition to their inherent complexity, the traditional properties of standard peripheral interconnects like PCIe have until recently led accelerators to avoid participating in these coherence protocols, instead using a computational model like OpenCL or CUDA based on explicit or implicit copying of the data. However, even for CPU-only software, the complexity of such protocols and the difficulty of effectively optimizing performance for them have led to proposals for, e.g., operating systems that avoid requiring cache coherence [4] and communicate between cores via messages, which themselves are using the coherence protocol in unexpected ways [18].

### 2.2 FPGAS and Coherence Protocols

A recent trend is for accelerators to be made cache-coherent with the CPUs in a heterogeneous system. We focus on FPGA-based accelerators, but the trend with GPUs is similar [34].

Xilinx Zynq Ultrascale+ [50] and Intel Agelix [22] are embedded Multiprocessor System-on-chip (MPSoC) architectures that combine a CPU and FPGA on a single die, simplifying the interconnect and offering both coherent and non-coherent ports between the two. Coherent access is generally asymmetric, and limited to allowing the FPGA to access the CPU’s last level cache.

Two examples of an Field Programmable Gate Arrays (FPGAs) connected coherently with an asymmetric protocol are Intel’s HARPv2 system [36] and IBM’s CAPI [46]. In HARPv2 a 14 core CPU is connected coherently to an FPGA via Intel’s Quick Path Interconnect (QPI). Although QPI supports a symmetric protocol [14], the FPGA implements only a caching agent. The coherence protocol is configurable via a cache coherence table but no information is available on how to modify the protocol. IBM’s CAPI system combines a 12 core processor asymmetrically with an FPGA. This system is built on top of PCIe interconnect with coherence being enabled by a PCIe Host Bridge (PHB) and Coherent Accelerator Processor Proxy (CAPP) on the processor and a POWER service layer (PSL) on the FPGA. Both systems provide a unified addressing space for applications on the FPGA.

The need to coherently connect heterogeneous accelerators to CPUs has led to several recent interconnect standards. CXL [15] builds coherence and memory semantics on top of a PCIe transport. It provides a unified coherent memory space between host CPU and accelerators, using an asymmetric protocol on the accelerator with a coherence bypass to allow direct access to unshared parts of device memory. OpenCAPI [45] also implements an asymmetric protocol over PCIe (and, more recently, Bluelink). Accelerators are required to work with caching enabled and virtual addresses, with virtual to physical mapping done by the CPU’s MMU. CCIX [9], on the other hand, supports a symmetric protocol on the accelerator by extending PCIe. This enables accelerators to work as peer of the CPU in an unified, coherent memory space.

The above examples favor near-memory processing where accelerator memory expands CPU system memory. GenZ [17] instead supports both near- and far-memory processing by defining memory semantics for communication between CPUs, accelerators, and memories. GenZ is designed to scale to entire racks. It does not specify operation of the cache coherent agent but specifies protocols that support building these agents.

In practice the role of the FPGA in a coherent CPU-FPGA system depends on the protocol implemented in the FPGA. *Asymmetric* protocols mean the CPU and FPGA have a host-device relationship where the CPU implements both home and caching agents and FPGA implements only the caching agent. To access pages in FPGA memory that are marked as shared with the CPU, the FPGA has to make a request to the CPU which maintains coherence. In contrast *symmetric* protocols enable CPU and FPGA to function as peers by implementing a home and caching agent on both, exactly as in a homogeneous NUMA system. The rationale for asymmetric protocols is that the critical access class for the FPGA is from device engine to device memory, and data can be copied in bulk in advance of computing on it. Symmetric protocols provide a seamless integration between the CPU and FPGA but are naturally more complex to implement. Both classes, however, as still “all or nothing” cache coherence protocols.

## 2.3 Accelerated Applications

There has been a massive proliferation of hardware accelerators with different models of execution. The initial generations of accelerated applications focused primarily on the host-device computational model where a host CPU is responsible for allocation and scheduling of accelerator resources on external devices. In this familiar execution model, data is offloaded in bulk, often via PCIe, for processing and the results are returned to the host. This remains the primary operation mode of GPU-accelerated applications (e.g. CUDA [35] and OpenCL [44]), as well as more modern application-specific hardware accelerators such as TPUs [25] and VCUs [39]. This model of execution has not shown much need for cache coherence, not least because of a historical lack of hardware caches and shared memory. However, more generally, the fixed nature of execution provides for efficient structured offloading, splitting execution evenly between host and device. Implicit acceptance of this model can be seen in the use of OpenCL to program FPGAs, thereby reinforcing the bulk data loading model for accelerators.

## 3 ECI DESIGN

### 3.1 Systems Overview

The design of ACCI is driven by the emergence of the application classes above, executing largely non-CPU devices, but which would nevertheless likely benefit from coherence. That these are *not* CPUs informs our choice to emphasize flexible protocol subsetting and to expose low-level primitives: Firstly (in combination with Enzian) to drive the exploration of suitable coherence models, and secondly as a recognition that specialised hardware may well need specialised protocols.

ACCI is carefully designed to interoperate cleanly with an existing native coherence protocol to allow realistic evaluation of server-scale workloads, while remaining scalable both down to specialized sub-protocols and up to new and more capable platforms. The implementation is (and will remain) a work in progress. To demonstrate what performance can be expected from a carefully-optimized implementation (and to show that it is competitive with the native protocol), we implement representative prototypes of several workloads in the currently best-optimized configuration: read-mostly operation offload to the FPGA, with results in section 5.

### 3.2 The Protocol

The ACCI design has several goals: First, to interoperate cleanly with the native coherence protocol of the ThunderX-1. Second, a clear specification *independent* of particular machine details. Third, to be fast. Fourth, to be extensible to new hardware. Last, it must be modifiable—in particular to allow protocol subsets for specific applications.

The ThunderX-1 implements a 2-node MOESI protocol with home-based directory. Compared to MESI, dirty lines are forwarded between caches without writing to RAM thanks to the O (dirty and shared) state. In a home-based system, consistency is the responsibility of a single node (the home), which is responsible for all reads from and writes to the backing store (e.g. RAM). If the remote holds a line in a ‘clean’ state (e.g. S), the home node ensures that the system behaves exactly as though the home node also held a

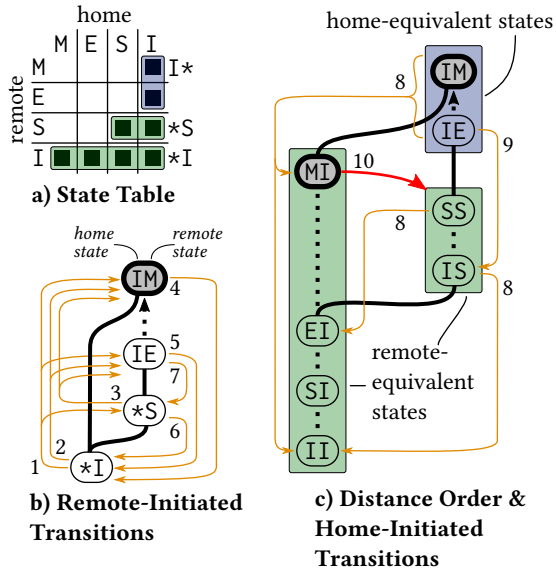


Figure 1: ECI protocol states and transitions

clean copy (S), or not at all (I). If home holds the line dirty (O), this is completely invisible the remote node.

Full MOESI is beyond what existing applications are likely to benefit from, and at the same time a very ambitious target for a first release. However, we do not exclude the option of extending ACCI to a full MOESI (or MESIF or any other protocol) in the future. For now, we opt for a compromise: Beginning with the native protocol on the ThunderX-1, we abstract the core features useful for current and near-future applications. We then generalize by specifying a core set of states and transitions that an implementation *must* support, and an envelope of things it *may*.

ACCI is specified as transitions and messages, agnostic to the underlying transport. On the ThunderX-1 this is a transport protocol guaranteeing reliable delivery, with multiplexed virtual circuits to guarantee deadlock freedom. The transport layer will naturally be dictated by the application scenario. It need only guarantee reliable delivery and a mechanism to avoid deadlock due to delivery order.

Likewise, the protocol envelope does not specify additional intermediate states (and associated messages) needed to handle message reordering and races. As described below, our reference implementation implements all intermediate states for CPU interoperability, but the user need only consider the specified *stable* states, even when working with a protocol subset.

### 3.3 Protocol Envelope

The home-node protocol of the ThunderX-1 gives a natural ordering of protocol states in terms of the ‘distance’ of data from its at-rest position (e.g. DRAM, or custom query logic for dynamically-generated data), shown in Figure 1.

As shown in Figure 1(a), we abstract the underlying MOESI protocol to an ‘enhanced’ MESI, with the standard set of allowable state pairs. The ordering relation between (joint) states is depicted

by thick black lines to states higher in the figure and connected by either a solid line (for globally-visible transitions) or a dotted line (for local transitions). The order is transitive, and thus IM (invalid at home, modified at remote) compares higher than II (invalid at both). Two transition classes exist: Upgrades, moving higher in the distance order (e.g. transferring from home to remote, or a line becoming dirty) and downgrades, moving downwards (e.g. writebacks).

States related only by local (dotted) links are indistinguishable to the other node, as indicated by shaded rectangles in Figure 1(a,c), with the exception that it may be possible to discover *after the fact* which state the other node was in after a transition e.g. transition 8 (downgrade remote to invalid) reveals whether the remote node held a dirty copy (by returning the dirty data) and may thus leave the home node with a line in either state M or I.

Figure 1(c) shows all possible combinations of home (left) and remote (right) states for a cache line e.g. IS where home node no copy (I), and remote holds a shared but clean copy (S). The thin orange arrows in this subfigure depict the minimal set of transitions that the home node may generate, and the remote node must therefore support. These are the *home-initiated* transitions, and only include downgrades: in the current protocol there is no mechanism to transfer data to a remote node without that node first requesting it. This restriction is necessary so that the baseline specification is satisfied by the ThunderX-1, which lacks any such mechanism.

It is permissible for a node to support more transitions than the minimal subset. For example, ‘downgrade remote to invalid and forward’ which would add a transition from state IS to state SI is *not* included in the minimal protocol (and indeed does not exist on the ThunderX-1), but would be a potentially useful extension (to avoid a read from RAM) that an extended implementation might support while remaining consistent with the basic rules.

Another transition excluded from the minimal (MESI) protocol is that labeled 10 (and coloured red) in Figure 1(c), from MI to SI or IS. This case occurs when a remote node wishes to upgrade its copy to the shared state (i.e. to read it), but it’s held dirty by the home node. This is where the basic MESI protocol is forced to unnecessarily write the dirty data to RAM rather than simply forwarding between caches, and is the primary advantage of MOESI. This transition is allowed by the ThunderX-1, as its native protocol is actually MOESI, and thus includes the 0 (owned, dirty and shared) for exactly this case. We permit this transition as a concession to performance, with the requirement that whether the home node’s copy is dirty or clean must be strictly invisible to the remote node. Whether the home node internally uses the 0 state or silently writes the dirty data back must not be visible.

From the ordering on states we derive the following *requirements* for allowable transitions:

- (1) A transition may only occur from a lower to a higher state, or higher to lower. Transitions between unrelated states e.g. (IE and MI) are forbidden. There is one exception (transition 10), as described above.

| Initiated by | Transition class | Transition Request               | Request has Payload | Response from Partner | Response has Payload |
|--------------|------------------|----------------------------------|---------------------|-----------------------|----------------------|
| Remote       | Upgrade          | Read-Shared                      | No                  | Yes                   | Yes                  |
| Remote       | Upgrade          | Read-Exclusive                   | No                  | Yes                   | Yes                  |
| Remote       | Upgrade          | Upgrade from Shared to Exclusive | No                  | Yes                   | No                   |
| Remote       | Downgrade        | Downgrade to Shared              | Yes if dirty        | No                    | No                   |
| Remote       | Downgrade        | Downgrade to Invalid             | Yes if dirty        | No                    | No                   |
| Home         | Downgrade        | Downgrade to Shared              | No                  | Yes                   | Yes if dirty         |
| Home         | Downgrade        | Downgrade to Invalid             | No                  | Yes                   | Yes if dirty         |

**Table 1: Signalled Transitions.**

- (2) Any transition between states distinguishable to the other node must be signaled i.e. an by exchange of messages. A reply is only required if necessary for consistency. Transitions over only internal (dotted) edges need not be signaled.
- (3) Moving from a dirty to a clean state *must* involve signaling the home node. This means the edge from IE to IM may only be traveled upward (as indicated by the arrowhead). The only downgrade path is thus via the MI path on the home node.
- (4) States where the remote node holds a clean, shared copy *must* be indistinguishable to the remote node. If the home node holds dirty data, this must be entirely invisible to the remote (hidden 0 state).
- (5) Implementations *must not* signal transitions not supported by the interoperating node. This rule is in practice mostly used in the converse: an implementation must support all transitions the partner may signal, unless it can be guaranteed these won't be generated (e.g. with a read-only workload).
- (6) Any transition a node is permitted to request in a given state must also be permitted in any other state indistinguishable to that node (i.e. reachable by silent transitions of the other node).
- (7) A node in a given state must be prepared to receive any message that it would be prepared to received in any indistinguishable state.

To ensure reasonable performance, implementations should follow the following *recommendations*:

- (1) Internal transitions *should not* be signalled, particularly upgrades to dirty states (e.g. IM).
- (2) The home node *should* avoid writing dirty lines before sharing them. This *must* be done in a manner invisible to the remote node.

As already discussed, Figure 1(c) provides the minimal set of home-initiated transitions plus MOESI-like remote-initiated transition 10. Transition 9 is requested by 'downgrade remote to shared', while the three transitions labeled 8 are triggered by 'downgrade remote to invalid'. Where the current state is SS or IS, the new home state is either E (home now has the only copy) or I, respectively. In these cases, the home knows which transition will occur (it can distinguish the two states). The home node cannot distinguish IM and IE however, as the upgrade to IM is silent. The final state (either IM or II) is thus only apparent when the remote node replies, either

with dirty data or without. For all home-initiated downgrades, the remote node must reply so the home node can distinguish remote I, S and E/M to maintain coherency. Table 1 lists all signaled home and remote transitions.

Figure 1(b) shows the possible joint states from the perspective of the remote node, with the remote-equivalent states merged into the combined states \*S and \*I. Requirement 6 guarantees that this is sound, and with requirement 7 that the remote node need only implement this 4-state protocol. The left-hand side of the figure shows the mandatory remote-initiated upgrades: Invalid to shared (1), invalid to exclusive (2), and shared to exclusive (3). The right-hand side gives the remote-initiated downgrades: Modified to invalid (writeback) (4), exclusive to invalid (5,6), and exclusive to shared (7).

The MOESI downgrades 'modified to shared' and 'exclusive to shared' are not part of the minimal protocol (although the ThunderX-1 does permit them). A consequence of requirements 6 and 7 is that remote-initiated ('voluntary') downgrades to either shared or invalid do not require a reply from the home, as the remote need not distinguish the possible home states.

### 3.4 Specialization

ACCI is explicitly intended to be modified to suit particular applications. Figure 2 illustrates three examples: (a) an FPGA-implemented accelerator that interacts with the CPU principally as a DMA initiator; (b) a fully-coherent symmetric two-node system (FPGA & CPU); and (c) a 'smart memory controller' system where most transactions are initiated by the CPU.

Each of these use cases makes different demands on the coherence protocol, and allow various optimizations and simplifications. Indeed, for the CPU-initiator case and a read-only workload, the number of states needed to be distinguished on the host node (the FPGA for workloads such as operator pushdown) is one, and the FPGA accelerator can remain coherent despite implementing neither cache nor directory! We demonstrate this optimization is safe, and evaluate its performance in section 5.

Refer again to Figure 1(b), and consider a read-only workload. For the remote node (here the CPU), the IM and IE states do not occur, leaving only \*S and \*I. Only transitions 1 (upgrade to shared) and 6 (voluntary downgrade to invalid) remain. Appealing to requirement 5, the home node (FPGA) need only respond to the upgrade (which requires a reply) and the downgrade (which doesn't).

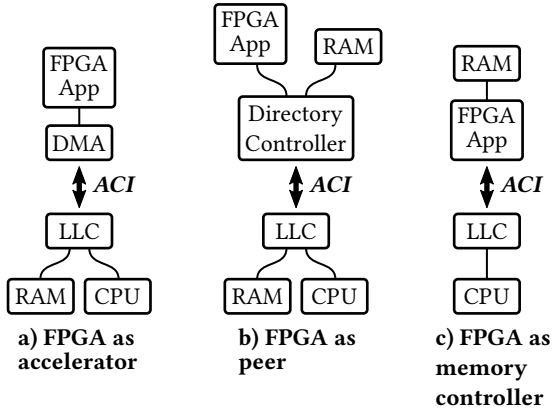


Figure 2: Instances of ECI specialization

Turning to Figure 1(c), we can immediately discard states MI, IM, and IE and the associated transitions (9, 10, and one case for 8). If the FPGA does not locally cache the data (it will be cached on the CPU, the FPGA will never need to deal with a dirty line), then the EI, SI, and SS states likewise vanish, leaving only a two-state protocol consisting of IS and II and the host-initiated downgrade to invalid transition (8). The only reason for this one remaining home-visible transition is to evict data known to be clean, and it too may be discarded, leaving only the combined state  $I^*$  (uncached at home, remote state shared or invalid) and no host-initiated transitions. The FPGA-side home node need only respond to ‘upgrade to shared’ requests with the necessary data, and silently ignore voluntary downgrades from the CPU: neither requires transitioning from  $I^*$ , and thus the FPGA need track no state at all for a cache line.

Note that this dramatic simplification does not impact the CPU’s ability to cache the data (often generated at great cost in time and energy by an accelerator). As section 5 shows, not only does the simplified endpoint interoperate flawlessly with the ThunderX-1, the performance of workloads with significant temporal locality increases dramatically thanks to transparent use of the CPU’s L1 and L2 caches.

## 4 THE ECI TOOLKIT

ACCI is based upon the existing ThunderX-1 coherence protocol. Despite excellent support from the CPU vendor in the form of documentation and conversations with the designers, coherence on the ThunderX-1 was never designed (or documented) with a heterogeneous system use-case in mind – the design goal was for two identical CPUs to talk to each other in a 2-socket homogeneous system. We used a combination of tracing technologies, ad-hoc trace analysis tools, formal specifications of different protocol layers, and simulation techniques to help both in implementing ACCI and also as a subsequent aid for developers using it. These tools are available to make it easier to explore ACCI in detail.

### 4.1 Supporting tools

**Trace capture:** We started by gathering a set of reference traces from two ThunderX-1 systems configured in a 2-socket NUMA

configuration booting Linux from power-on up to the shell prompt. By interposing an FPGA board between the two cores, and reducing the number of 10 Gb/s lanes used by the coherence protocol, we were able to capture bidirectional traces at the block level and download them to a PC for analysis.

From these low-level traces we constructed the sequence of coherence messages in each direction on all virtual circuits used by the protocol. We defined our own JSON-based serialization format for these messages along with a canonical binary format, ECI Wire Format (EWF), to allow the decoded traces to be used for a variety of purposes. We also wrote a plugin for the popular Wireshark protocol analysis tool [48] for visualizing the protocol.

**Formal specification and modelling:** Our evolving view of ACCI was captured in a set of formal specifications which we checked against our traces. One of these used the SAIL specification language [2] for specifying the format of the individual messages – indeed, the code for decoding these messages into our serialization format was generated from this specification.

A second specification captured the valid protocol message exchanges. A cache coherence protocol often has many outstanding transactions. We used this spec against our traces to check that our state machines were consistent with the observed behavior of the native protocol – when they disagreed, we reworked our specification.

It should be noted that the protocol itself does not simply consist of coherence-related messages. Non-cacheable I/O accesses, memory barriers, and interprocessor-interrupts are all carried via this protocol.

A third specification attempted to capture the actual coherence protocol itself: state transitions for cache lines, intermediate states when messages were in flight, etc. Here we were helped by considerable prior work on specifying cache coherence protocols in academia, and the fairly clean nature of the protocol we were modeling. The resulting specification was a considerable superset of that required for ACCI, and covered 4-node NUMA systems.

**Simulation:** Given “legitimate” traces of messages and a standard format for representing these in software, we could now simulate either end of an ACCI link. For the FPGA side, we used a standard Verilog simulator in place of the FPGA to send and receive ACCI messages using our evolving ACCI implementation.

For the CPU side, we implemented a custom cache module in C++ for the ARM Fast Model simulation suite [1] which modelled the ThunderX-1 L2 cache. This allowed us to run application binaries over Linux as if on the Enzian CPU, but our cache module would also send and receive ACCI messages correctly (modulo our specification) over a network socket using our JSON format and adjust the cache state accordingly.

Connecting these two over TCP sockets provided a viable simulation environment for the entire machine, useful not only for debugging ACCI itself, but also for those developing both software and FPGA applications.

**Online tracing:** One deficiency of using offline reference traces to guide the implementation is that rare, unusual events are sometimes missing from the traces. Failing to react on the FPGA side to these events often caused a machine check on the CPU, with very little information available as to why.

**Table 2: ACCI hardware resource consumption, percentage over the resources available in a Xilinx VU9P**

|               | LUTs  | REGs  | BRAM(36Kb) |
|---------------|-------|-------|------------|
| ACCI per link | 46186 | 32777 | 112.5      |
| Percentage    | 3.91% | 1.39% | 5.23%      |

In addition to the On-Chip Logic Analyzer (OCLA) on the FPGA, we developed a tool for online tracing of ACCI which could check parts of our protocol specification against a running Enzian system at the full link rate of 240 Gb/s and record violations of our specification.

The parts of the protocol to be verified are specified as Nondeterministic Finite Automata (NFAs) using a simple language, which is compiled into a circuit synthesized on the FPGA along with the rest of the FPGA configuration. Loading a new configuration takes only a few seconds, whereas resynthesising a specialized engine can take many hours. The tool requires modest FPGA resources, yet can capture complex events at full line rate without any additional latency. It can thus be used to debug and analyze the behavior of very high-speed interconnects without interrupting execution, enabling the observation of transient, complex events in real time, and has proved invaluable in ironing out the remaining interoperability corner cases in ACCI, as well as debugging applications using it.

## 4.2 Reference FPGA Implementation

The reference implementation of ACCI is inter-operable with ThunderX-1 CPUs, open, and reconfigurable. The implementation is layered: virtual channel (VC) layer, link layer, transaction layer and physical layer. The VC layer implements 14 different virtual channels that expose Input/Output (IO) and coherence operations to the FPGA, of which 10 are for coherence traffic, with separate sets of VCs for odd and even cache lines enabling simpler load-balancing. In order to provide a deadlock free network, the current implementation of the VC layer is based on the message classes defined by ThunderX-1 and can be reconfigured as necessary.

There are no ordering guarantees across VCs and the implementation thus handles race conditions using additional intermediate states, invisible to the application. The link layer formats coherence messages and efficiently packs them for transport through lower layers. The transaction layer manages link state, credit based flow control, and error and replay mechanisms to ensure delivery of messages. The physical layer is responsible for transport of ACCI messages through serial lanes. All these layers have been tested and have good performance. In addition, ACCI needs very few resources on the FPGA, leaving plenty of room for the application (Table 2)

The FPGA can choose to implement asymmetric or symmetric versions of the coherence protocol and reference designs are available for both. To support the 2-node symmetric model where the CPU and FPGA operate as peers with respect to the coherence protocol, an a directory controller implementation is available which implements a state space that can be tailored to needs of different applications. For example, the reference implementation of the protocol is tailored towards expanding the CPU’s memory by being able to access the FPGA’s memory coherently. Though not present

in the reference implementation, the FPGA can choose to implement a cache or interact directly with the directory controller to access both CPU and FPGA’s memory. The directory-controller’s entire state machine, including intermediate states to handle race conditions, is generated automatically from a formal specification. For reasons of space, we do not discuss the directory controller implementation any further in this paper but the code is available.

In this paper we explore in more detail the 2-node asymmetric configuration, turning the FPGA into a custom memory controller implementing near-memory-processing operators. In this use case, the FPGA interacts directly with the coherence protocol to function as a custom memory controller providing different coherent views of the device memory to the host and placing the data directly on the L2 cache of the requesting core. We use this use case to illustrate the performance that can be expected from a fully-optimised implementation of ACCI on an FPGA and its versatility in practice. In this design, the FPGA reads its memory on behalf of the CPU but it implements high level operators that process the data in flight between the FPGA memory and the CPU cache. We have implemented three operators corresponding to common FPGA-offload scenarios in the literature: an SQL SELECT operator pushdown where the FPGA filters data according to a simple predicate, a pointer chasing operator that can traverse data structures to find the relevant data items, and a regular expression matching engine that is used to filter data before sending it to the CPU. These are all instances of topology c of Figure 2, this being the most mature of our reference implementations, already achieving close to the theoretical performance limit. All three workloads take advantage of the optimizations permitted by the specialization described in subsection 3.4.

## 5 EVALUATION

We show, first, that ACCI’s flexibility has essentially no cost, and that we can implement full coherency on the FPGA. Next, microbenchmarks show performance as close to the CPU’s native implementation as is likely possible using an FPGA. Finally, macrobenchmarks implementing operators in the memory controller illustrate the design and provide examples of how ACCI can be employed in practice.

### 5.1 Hardware Platform

We use the recently-released Enzian research computer [12] as our experimental platform:

- CPU: Marvell ThunderX-1, 48x dual-issue ARMv8, 2.0GHz, 16MB 16-way associative LLC, 128B lines.
- CPU DRAM: 4x 32GiB 2133MT/s DDR4 channels (only 2 used)
- FPGA: Xilinx Ultrascaleo+ XCVU9P at 300MHz.
- FPGA DRAM: 4x 16GiB 2400MT/s DDR4 channels (only 2 used)
- Interconnect: 30GiB/s bidirectional (theoretical, including overheads).

|             | Enzian + ACCI | 2-socket server (native) |
|-------------|---------------|--------------------------|
| Throughput: | 12.8 GiB/s    | 19 GiB/s                 |
| Latency:    | 320 ns        | 150 ns                   |

Table 3: ACCI performance comparison

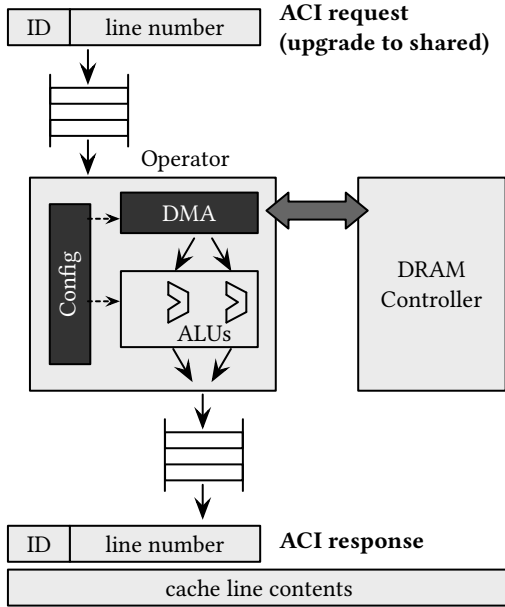


Figure 3: The common structure of experimental operators

## 5.2 Microbenchmarks

We first look at the performance of ACCI as an inter-socket interconnect. The key question is whether coherency protocols implemented on FPGAs can realistically interoperate with native CPU implementations.

We compare throughput and latency of inter-socket cache operations on Enzian with an off-the-shelf conventional 2-socket server machine with the same CPUs, which provides an upper bound on the achievable performance of ACCI.

The result in Table 3 shows that, while our current ACCI implementation could undoubtedly be further optimized, these results do show that ACCI exhibits realistic performance for cache coherence hardware. Note that the FPGA has a much lower clock speed than the CPU and, as a result, it will always be intrinsically slower than a CPU executing the same protocol. Nevertheless, we believe that further optimizations are possible that will reduce the gap between the CPU and the FPGA implementation.

## 5.3 Experimental Setup

**5.3.1 Operator interface via ACCI.** The FPGA portion of all three workloads is implemented according to the structure depicted in Figure 3. The operator receives commands as requests over ACCI: specifically, requests to upgrade a cache line to the shared state. For the select pushdown and regex operators the line number (i.e.

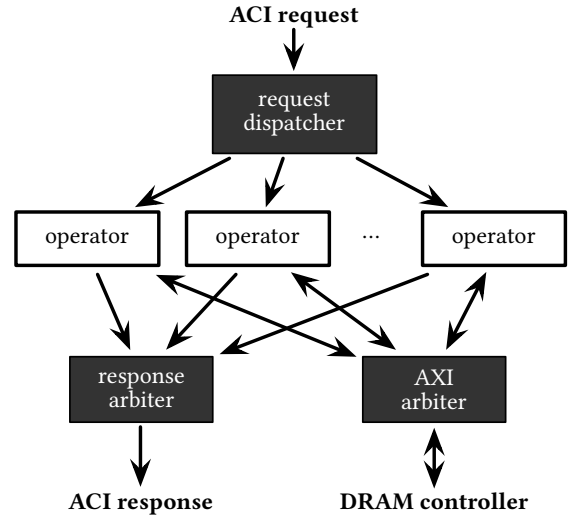


Figure 4: Parallel operator pipeline

read address) is unused, as both return results FIFO. For the pointer-chasing workload the address is hashed to identify a bucket in which to search for a key.

The main data flow through the operator is from FPGA-side DRAM via an integrated DMA engine, through the arithmetic units, and out to the CPU’s LLC (L2 for the ThunderX-1) as a response to an upgrade request. The request flow is from the CPU (as upgrade requests), through the DMA engine and arithmetic units, and back as an ACCI response. From the CPU perspective, the performance-critical portion of the workload is read-only, with the FPGA acting as a ‘smart’ memory controller, performing data reduction and/or computation as appropriate. Data is carefully packed to make efficient use of cache-line-sized transfers (128B).

Each operator is configured by read/write access (also over ACCI) to a *config* module, e.g. to set query parameters or to load a regex. This communication is not on the critical path of the workload, and is not included in our measured results.

The CPU cores are mostly in-order, and thus tend to serialize very quickly in the presence of significant latency, which grows as the FPGA does more work. Thus performance scaling is mostly achieved (as the ThunderX-1 designers intended) through parallelization across the many cores. Both the ACCI implementation and our operators are highly concurrent, and service a large number of results in parallel using multiple arithmetic units. The principal scaling parameter in our experiments is thus CPU thread count.

**5.3.2 Hardware interface for multi-operator design.** Some workloads, including our pointer-chasing example, are heavily constrained by the latency of outstanding DRAM requests, which take ~100ns on Enzian. The 512b interface provided by the DRAM controllers limits such an operator to ~640MB/s throughput.

To achieve higher performance, it is necessary to run multiple parallel operators, as shown in Figure 4. Here, ACCI requests are fanned out by a central dispatcher to many operators, each incorporating a DRAM controller. This structure is used in the pointer-chasing workload.



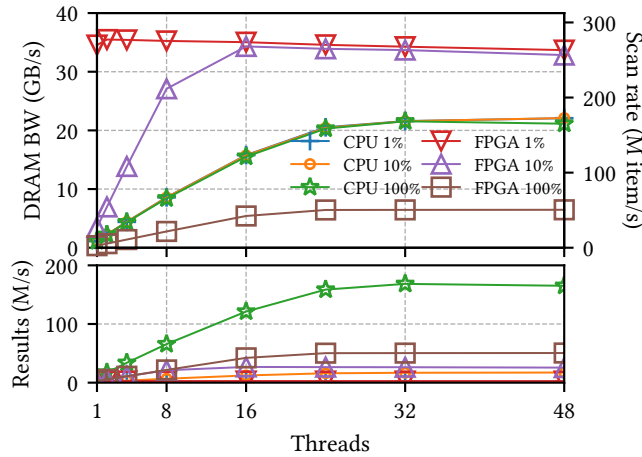


Figure 5: SELECT throughput vs. selectivity and thread count for CPU and FPGA implementations.

#### 5.4 SELECT pushdown

The first operator we explore in the FPGA based memory controller is an SQL’s SELECT operator that filters data according to a simple predicate. It demonstrates the overall performance improvement obtainable for data-reduction operators with little or no compute by limiting the amount of data moved across the machine. It also shows the advantages of ACCI for building applications. Because the filtering is transparent, the CPU only issues a read operation to a particular address. This mechanism reflects the *volcano execution model* used in relational engines where tuples are passed from an access method to the rest of the query plan through a series of *next* calls. With ACCI, the access method implementing the selection is pushed down to the memory controller on the FPGA with matching tuples passed on to the CPU LLC.

The operator supports queries of the form SELECT \* FROM S WHERE S.a > X AND S.b < Y, a and b are two attribute values of row S, which is sized to fit within a cache line. The operator performs a table scan when triggered by a read from the CPU to a FIFO address, and returns matching rows in order upon receiving further reads. Multiple cores may safely read the FIFO concurrently once the scan is initiated, and will receive interleaved results. Matched rows are pushed to an output FIFO and returned on a first-come first-served basis. The operator is fully pipelined. The table contains 5120000 rows (655 MB). We vary selectivity, the proportion of returned records, to show the effect of bottlenecks in different components.

Figure 5 presents the throughput for selectivity 1%, 10%, and 100% against thread count. The measured quantities are scan rate (rows/second) and DRAM read bandwidth (which is proportional) in the top plot, and results returned per second in the lower. The CPU curves are for an operator running entirely on the CPU with data in CPU DRAM, while the FPGA curves are for an operator initiated by the CPU but executed on the FPGA with data in the FPGA DRAM.

The scan rate on the CPU is independent of selectivity, and is limited by the CPU’s DRAM bandwidth. The FPGA’s scan throughput depends strongly on selectivity: Where the fraction of matching

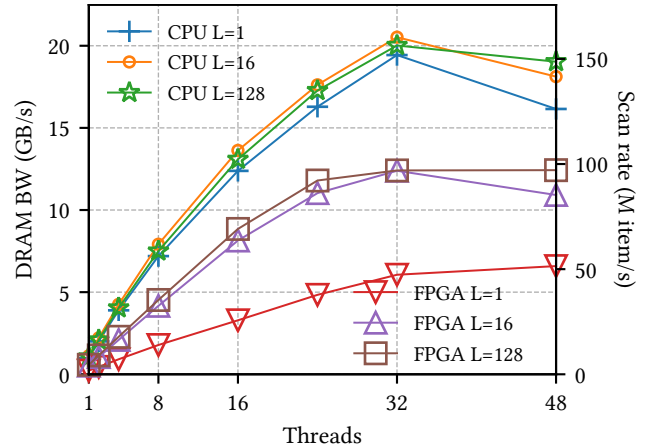


Figure 6: Pointer-chasing throughput on CPU and FPGA for varying chain lengths.

results is less than the ratio of interconnect bandwidth to FPGA DRAM bandwidth (1 : 6 here), the FPGA operator is limited only by DRAM bandwidth once enough threads are running to keep the pipeline full (16 for 10% selectivity). Once selectivity is high enough to saturate the interconnect (e.g. at 100%) the scan behaves as the CPU implementation, albeit with the reduced bandwidth to remote DRAM.

The curves for results per second show an inversion for high-selectivity queries, as we would anticipate from the scan rate. When most of the data is returned to the CPU, higher bandwidth to local DRAM becomes dominant. For lower selectivities, i.e., where there is an effective data reduction, the FPGA-offloaded operator achieves higher performance, and at a lower CPU thread cost.

#### 5.5 Pointer chasing in a key-value store

The second operator we implement in the memory controller tests the utility of offloading a latency-bounded operation: pointer chasing, to the FPGA. The workload is a key-value store (KVS) implemented as a hash table with separate chaining. A key (encoded in the address sent over ACCI) is hashed to select a bucket, which contains the head pointer to a linked list of key-value pairs. Each (read) request from the CPU triggers a pointer chase along the linked list to locate the matching key. Each CPU core will block waiting for a result, and parallelism is achieved through multiple outstanding requests, using the multiple-operator architecture described in Figure 4.

Each list entry is 128B, comprising an 8B key, 112B value, and 8B pointer to the next entry. The KVS contains 5120000 key-value pairs, uniformly distributed between buckets. To simulate different table fill states we vary the chain length and search for the last key in the list to force a known-length pointer chain. The FPGA implements 32 parallel operators.

Figure 6 shows the throughput of the pointer chase operator, with DRAM bandwidth on the left and keys/second on the right. The chain length varies from 1 to 128. Clearly, this is a negative

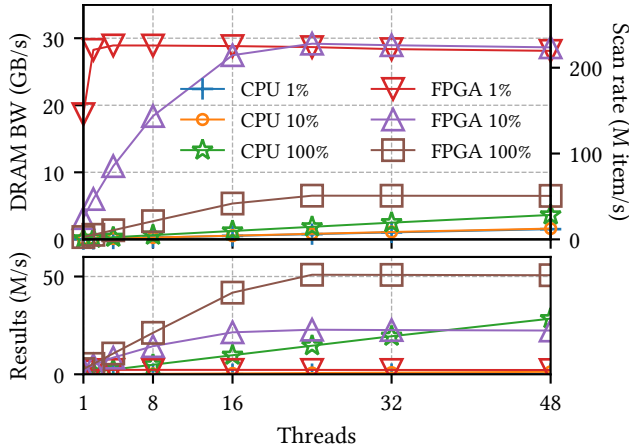


**Figure 7: Regular expression throughput vs. thread count and selectivity for CPU and FPGA.**

result for this particular workload, but a success for ACCI as a prototyping system: We could quickly determine whether a seemingly-promising accelerator would perform well in practice. The limiting factor here is the random-access performance of the DRAM subsystem for both CPU and FPGA, and here the CPU has an advantage with its large cache, higher clock frequencies, and carefully-tuned design. The length-1 curve for the FPGA shows again the effect of interconnect saturation, as the number of DRAM accesses per ACCI transaction is 1.

## 5.6 Regular expression matching

The final operator we consider integrates an open-source regular expression matching engine [23, 42, 43] into the memory controller. This extends the SELECT operator of the first experiment to support more sophisticated filters, namely SQL’s REGEXP LIKE, which implements text search over strings using regular expressions. While still filtering data, the regex match is dramatically more computationally intensive, which consequently changes the workload characteristics. This workload thus stands in for the general offloading of *compute-intensive* operations.

The operator works on a 62B string field within the 128B row, and takes one cycle-per-character, fully pipelined. Mismatches terminate early. As it was the case for the SELECT experiment, the operator performs table scans on behalf of the CPU, with matching rows returned in a FIFO from which cores read concurrently. The table again contains 5120000 rows, and the FPGA uses 48 parallel matching engines. We seed the table with a set number of matching strings to control the query selectivity. The CPU-only implementation uses a well-optimized open-source library [29].

Figure 7 shows the throughput results, reported as for previous experiments. The overall pattern is essentially the same, except that thanks to high computational intensity, and that regex matching is particularly well-suited to FPGA implementation, the FPGA-offloaded version outperforms the CPU in every case, even when there is an interconnect bandwidth bottleneck in the 100% selectivity case. The FPGA implementation achieves twice the performance of the CPU version (operating on local DRAM) even when every

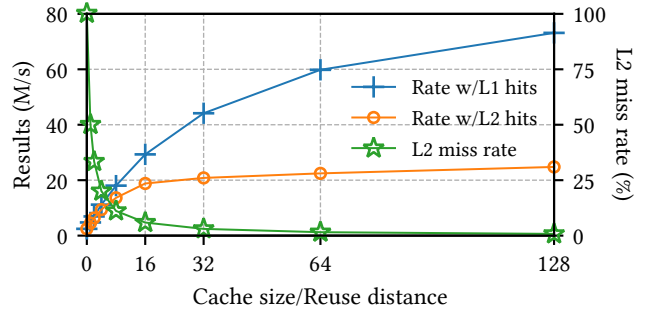


**Figure 8: The effect of temporal locality with ACCI**

result matches and must, thus, be sent to the CPU. This excellent throughput is achieved with only a third of the CPU cores involved (and it is mostly stalled on memory cycles).

## 5.7 Exploiting temporal locality

The results of all the operators are delivered to the CPU’s L2 cache in a manner completely invisible to both the CPU software and the operator itself, thanks to ACCI integration. If a result delivered to the CPU is expensive to compute in time or energy, reusing rather than recomputing it represents a significant saving.

To demonstrate the ease with which this can be achieved, with dramatic performance improvements, we took the baseline regex-matching scan of the previous experiment, and simulated an enclosing application with varying degrees of temporal locality. Instead of iterating through the scan once, we arrange that when the CPU reads value  $N$ , it will also re-read value  $N - D$ ,  $N - 2D$ , and so on, up to the size of either the L2 or L1 cache, as appropriate. We can thus directly control the degree of result reuse, which in this example are computed at great cost.

Figure 8 shows the result, with controlled parameter  $D$  as a fraction of the cache size, approximately equal to the number of times a result will be reused (modulo boundary effects and cache pollution). We report two different series: one each spanning the L1 and L2 cache sizes. For the L2 case, we plot the miss rate reported by CPU performance counters. All data was collected with one thread and a selectivity of 10%.

As can be easily seen, the effect is dramatic, with a single core outperforming the entire system at a reuse rate of 16 in the L2 cache, and 8 in the L2. This experiment illustrates the potential of fine-grained coherence for CPU-FPGA applications, and the benefits that a flexible low-level interface such as ACCI can deliver.

## 6 RELATED WORK

Cache coherency is well studied in architecture and systems; here we focus on work targeting access and customization of the protocol for accelerators in different settings.

Berg showed (for coherence between CPU and device) the benefits of different coherence modes (software, hardware, application-controlled scratchpad) vary significantly with application and system characteristics and thus no single protocol is necessarily “correct” [5]. This observation, albeit based on traditional I/O-based devices, agrees with our contention that in non-CPU-like devices,

the ideal coherence protocol depends on the application, with accelerators, the execution unit.

For FPGA SoCs, cache coherency has been studied using Networks-on-Chip (NoCs) [19, 20]. For example, the Zynq MPSoC provides the AXI-based ARM Coherency Port (ACP) interface which allows for coherent accesses using the ARM Snoop Control Unit (SCU). Sadri *et al.* use this to evaluate power/performance tradeoffs in various configurations of an image processing application [41]. Similarly, TileLink [13] is a chip-scale interconnect protocol for RISC-V processors providing coherent access to shared memory, using a customizable, MOESI-equivalent protocol optimized for tightly-coupled, low-latency SoC buses. These single-chip platforms target rather different use cases to the heterogeneous CPU-FPGA platforms we address. While they also open up the protocol, ACCI is an actual protocol stack fully compatible with the CPU coherence protocol, targeting server-class systems.

HARP was a server-class platform allowing coherent applications [36]. Unlike ACCI, HARP used QPI and only implemented an asymmetric protocol with limited access to the FPGA. Cabrera and Chamberlain ported OpenCL kernels from PCIe-based platforms to HARP, showing the benefits of shared virtual memory over explicit reads and writes [7]. The Centaur shell for HARP is a framework running hybrid relational queries, dynamically allocating FPGA operators to query plans [38]. Moreover, machine learning applications [3, 37] demonstrated coherence-related speedups on HARP over CPU-only implementations. These show the advantages of FPGA participation in the coherence protocol, which can be enhanced by the FPGA actively participating in a symmetric protocol, as with ACCI.

C-API (see subsection 2.2), is another asymmetric protocol allowing the accelerator to cache data. Ito and Ohara build a bioinformatics algorithm (pair-HMM) on a C-API-enabled system, achieving 33x better power-performance than with a POWER8 CPU alone [24]. They conclude that coherence between CPU and accelerator makes programming simpler and more efficient than with traditional accelerator design, a finding echoed by Mughrabi *et al.* accelerating PageRank algorithms by leveraging coherent caching on the FPGA [33]. Van Luntern *et al.* accelerate stencil processing using both a FPGA and ASIC in tandem with POWER9 [49] via OpenC-API. These all show significant power and performance benefits of various coherence models, while enabling programmers to use both existing and novel caching and threading techniques, and motivated our development of ACCI.

The use case we explore in this paper is similar to recent work on near-memory processing. Maas *et al.* [30] implement an on-die garbage collection accelerator for RISC-V processors connected to shared memory through TileLink. Similar functionality can be developed on ACCI without changing the processor architecture. This shows a fundamental difference between ACCI and protocols like TileLink: ACCI enables a reconfigurable accelerator to interact with the CPU at the coherence level, but crucially can be reconfigured on a per-application basis, whereas SoC or processor designs cannot be viewed as a dynamic component of the application: ACCI has been developed to support software applications rather than processor components.

Similarly, the ACCORDA [16] proposal for integrating a specialized SQL operator engine into the memory hierarchy, and the

Oracle SPARC M7 “Software in Silicon” accelerator, operate on the stream of data between DRAM and processor cache, while ACCI connects a programmable accelerator for arbitrary tasks to the coherent interconnect. Nevertheless, there are similarities which show the value of the functionality all these systems provide.

ACCI is the first design to provide a coherence stack fully compatible with a server-class CPU in a two-socket architecture, with few restrictions on the accelerator functionality - indeed, ACCI enables applications dynamically deployed on the FPGA tailor the protocol at runtime, transparently to the CPU.

## 7 CONCLUSIONS

ACCI is an open protocol implementation running on accelerators (currently FPGAs) and inter-operating with the CPU’s native cache coherence implementation. ACCI presents an abstracted view of the protocol to accelerator applications which allows subsetting the full protocol to achieve better performance and space efficiency, while insulating them from the full complexity of inter-operating with the CPU. ACCI has performance comparable to the original inter-CPU implementation with which it inter-operates, and we illustrate potential applications that benefit from ACCI.

Future work includes further ACCI implementation optimizations and exploring a number of intriguing scenarios enabled by ACCI: streaming data arriving from the network directly to the CPU cache, extending coherence across networks of FPGAs connected via RDMA, and using the cache coherence protocol as a way to extract runtime information on the memory access patterns of applications for automatic and dynamic tuning of the system.

## REFERENCES

- [1] ARM Ltd. Fast Models. <https://developer.arm.com/tools-and-software/simulation-models/fast-models>, August 2021.
- [2] Alasdair Armstrong, Thomas Bauereiss, Brian Campbell, Shaked Flur, Kathryn E. Gray, Prashanth Mundkur, Robert M. Norton, Christopher Pulte, Alastair Reid, Peter Sewell, Ian Stark, and Mark Wassell. Detailed models of instruction set architectures: From pseudocode to formal semantics. In *Proc. Automated Reasoning Workshop*, pages 23–24, April 2018. Two-page abstract. Proceedings available at <https://www.cl.cam.ac.uk/events/arw2018/arw2018-proc.pdf>.
- [3] Lukas On Arnold and Muhsen Owaida. Single-pass covariance matrix calculation on a hybrid fpga/cpu platform. In *EPJ Web of Conferences*, volume 245, page 09006. EDP Sciences, 2020.
- [4] Andrew Baumann, Paul Barham, Pierre-Evariste Dagand, Tim Harris, Rebecca Isaacs, Simon Peter, Timothy Roscoe, Adrian Schüpbach, and Akhilesh Singhanian. The Multikernel: A New OS Architecture for Scalable Multicore Systems. In *Proceedings of the ACM SIGOPS 22Nd Symposium on Operating Systems Principles, SOSP ’09*, pages 29–44, New York, NY, USA, 2009. ACM.
- [5] Thomas B. Berg. Maintaining i/o data coherence in embedded multicore systems. *IEEE Micro*, 29(3):10–19, 2009.
- [6] Amiralali Boroumand, Saugata Ghose, Minesh Patel, Hasan Hassan, Brandon Lucia, Rachata Ausavarungnirun, Kevin Hsieh, Nastaran Hajinazar, Krishna T. Malladi, Hongzhong Zheng, and Onur Mutlu. Conda: Efficient cache coherence support for near-data accelerators. In *Proceedings of the 46th International Symposium on Computer Architecture*, page 629–642, 2019.
- [7] Anthony M. Cabrera and Roger D. Chamberlain. Exploring Portability and Performance of OpenCL FPGA Kernels on Intel HARPv2. In *Proceedings of the International Workshop on OpenCL, IWOCCL’19*, New York, NY, USA, 2019. Association for Computing Machinery.
- [8] Irina Calciu, Ivan Puddu, Aasheesh Kolli, Andreas Nowatzyk, Jayneel Gandhi, Onur Mutlu, and Pratap Subrahmanyam. Project PBerry: FPGA Acceleration for Remote Memory. In *Proceedings of the Workshop on Hot Topics in Operating Systems, HotOS ’19*, page 127–135, New York, NY, USA, 2019. Association for Computing Machinery.
- [9] CCIX Consortium and others. Cache Coherent Interconnect for Accelerators (CCIX). <http://www.ccixconsortium.com>, January 2019.
- [10] Lucian M. Censier and Paul Feautrier. A new solution to coherence problems in multicache systems. *IEEE Transactions on Computers*, C-27(12):1112–1118, 1978.

- [11] Byn Choi, Rakesh Komuravelli, Hyojin Sung, Robert Smolinski, Nima Honarmand, Sarita V. Adve, Vikram S. Adve, Nicholas P. Carter, and Ching-Tsun Chou. Denovo: Rethinking the memory hierarchy for disciplined parallelism. In *2011 International Conference on Parallel Architectures and Compilation Techniques*, pages 155–166, 2011.
- [12] David Cock, Abishek Ramdas, Daniel Schwyn, Michael Giardino, Adam Turowski, Zhenhao He, Nora Hossle, Dario Korolija, Melissa Licciardello, Kristina Martensenko, Reto Achermann, Gustavo Alonso, and Timothy Roscoe. Enzian: an open, general CPU/FPGA platform for systems software research. In *Proceedings of the 27th ACM International Conference on Architectural Support for Programming Languages and Operating Systems, ASPLOS 2022*, pages 590–607, New York, NY, USA, 2022. Association for Computing Machinery.
- [13] Henry Cook, Wesley Terpstra, and Yunsup Lee. Diplomatic design patterns: A tilelink case study. In *First Workshop on Computer Architecture Research with RISC-V (CARRV 2017)*, 2017.
- [14] Intel Corporation. An introduction to the intel quickpath interconnect, Jan 2009.
- [15] CXL Consortium. Compute Express Link. <https://www.computeexpresslink.org/>, May 2020.
- [16] Yuanwei Fang, Chen Zou, and Andrew A. Chien. Accelerating Raw Data Analysis with the ACCORDA Software and Hardware Architecture. *Proc. VLDB Endow.*, 12(11):1568–1582, July 2019.
- [17] Gen-Z Consortium. Gen-Z Core Specification 1.1. <https://genzconsortium.org/>, August 2020.
- [18] John Giacomoni, Tipp Moseley, and Manish Vachharajani. Fastforward for efficient pipeline parallelism: A cache-optimized concurrent lock-free queue. In *Proceedings of the 13th ACM SIGPLAN Symposium on Principles and Practice of Parallel Programming, PPoPP '08*, page 43–52, New York, NY, USA, 2008. Association for Computing Machinery.
- [19] Davide Giri, Paolo Mantovani, and Luca P. Carloni. Accelerators and coherence: An soc perspective. *IEEE Micro*, 38(6):36–45, 2018.
- [20] Davide Giri, Paolo Mantovani, and Luca P. Carloni. Noc-based support of heterogeneous cache-coherence models for accelerators. In *2018 Twelfth IEEE/ACM International Symposium on Networks-on-Chip (NOCS)*, pages 1–8, 2018.
- [21] Daniel Hackenberg, Daniel Molka, and Wolfgang E. Nagel. Comparing Cache Architectures and Coherency Protocols on X86-64 Multicore SMP Systems. In *Proceedings of the 42nd Annual IEEE/ACM International Symposium on Microarchitecture*, page 413–422, 2009.
- [22] Intel. Intel agilex fpga product brief. <https://www.intel.com/content/www/us/en/products/docs/programmable/agilex-fpga-product-brief.html>, 2020.
- [23] Zsolt István, David Sidler, and Gustavo Alonso. Runtime parameterizable regular expression operators for databases. In *2016 IEEE 24th Annual International Symposium on Field-Programmable Custom Computing Machines (FCCM)*, pages 204–211. IEEE, 2016.
- [24] Megumi Ito and Moriyoshi Ohara. A power-efficient fpga accelerator: Systolic array with cache-coherent interface for pair-hmm algorithm. In *2016 IEEE Symposium on Low-Power and High-Speed Chips (COOL CHIPS XIX)*, pages 1–3. IEEE, 2016.
- [25] Norman P. Jouppi, Cliff Young, Nishant Patil, David Patterson, Gaurav Agrawal, Raminder Bajwa, Sarah Bates, Suresh Bhatia, Nan Boden, Al Borchers, Rick Boyle, Pierre-luc Cantin, Clifford Chao, Chris Clark, Jeremy Coriell, Mike Daley, Matt Dau, Jeffrey Dean, Ben Gelb, Tara Vazir Ghaemmaghami, Rajendra Gottipati, William Gulland, Robert Hagmann, C. Richard Ho, Doug Hogberg, John Hu, Robert Hundt, Dan Hurt, Julian Ibarz, Aaron Jaffey, Alek Jaworski, Alexander Kaplan, Harshit Khaitan, Daniel Killebrew, Andy Koch, Naveen Kumar, Steve Lacy, James Laudon, James Law, Diemthu Le, Chris Leary, Zhuyuan Liu, Kyle Lucke, Alan Lundin, Gordon MacKean, Adriana Maggiore, Maire Mahony, Kieran Miller, Rahul Nagarajan, Ravi Narayanaswami, Ray Ni, Kathy Nix, Thomas Norrie, Mark Omernick, Narayana Penukonda, Andy Phelps, Jonathan Ross, Matt Ross, Amir Salek, Emad Samadiani, Chris Severn, Gregory Sizikov, Matthew Snelham, Jed Souter, Dan Steinberg, Andy Swing, Mercedes Tan, Gregory Thorson, Bo Tian, Horia Toma, Erick Tuttle, Vijay Vasudevan, Richard Walter, Walter Wang, Eric Wilcox, and Doe Hyun Yoon. In-Datacenter Performance Analysis of a Tensor Processing Unit. In *Proceedings of the 44th Annual International Symposium on Computer Architecture, ISCA '17*, page 1–12, New York, NY, USA, 2017. Association for Computing Machinery.
- [26] David Kanter. The common system interface: Intel’s future interconnect. *Real World Technologies*, pages 1–4, 2007.
- [27] R. H. Katz, S. J. Eggers, D. A. Wood, C. L. Perkins, and R. G. Sheldon. Implementing a cache consistency protocol. In *Proceedings of the 12th Annual International Symposium on Computer Architecture, ISCA '85*, page 276–283, Washington, DC, USA, 1985. IEEE Computer Society Press.
- [28] John H. Kelm, Daniel R. Johnson, William Tuohy, Steven S. Lumetta, and Sanjay J. Patel. Cohesion: An adaptive hybrid memory model for accelerators. *IEEE Micro*, 31(1):42–55, 2011.
- [29] Kokke. A small regex implementation in c, 2021.
- [30] Martin Maas, Krste Asanovic, and John Kubiatowicz. A hardware accelerator for tracing garbage collection. *IEEE Micro*, 39(3):38–46, 2019.
- [31] Milo M. K. Martin, Mark D. Hill, and Daniel J. Sorin. Why on-chip cache coherence is here to stay. *Commun. ACM*, 55(7):78–89, 2012.
- [32] Michael R Marty. *Cache Coherence Techniques for Multicore Processors*. PhD thesis, University of Wisconsin-Madison, 2008.
- [33] Abdullah T Mughrabi, Mohannad Ibrahim, and Gregory T Byrd. Qpr: Quantizing pagerank with coherent shared memory accelerators. In *2021 IEEE International Parallel and Distributed Processing Symposium (IPDPS)*, pages 962–972. IEEE, 2021.
- [34] Vijay Nagarajan, Daniel J. Sorin, Mark D. Hill, and David A. Wood. *A Primer on Memory Consistency and Cache Coherence: Second Edition*. Morgan and Claypool, 2020.
- [35] John Nickolls, Ian Buck, Michael Garland, and Kevin Skadron. Scalable parallel programming with cuda: Is cuda the parallel programming model that application developers have been waiting for? *Queue*, 6(2):40–53, 2008.
- [36] Neal Oliver, Rahul R. Sharma, Stephen Chang, Bhushan Chitlur, Elkin Garcia, Joseph Grecco, Aaron Grier, Nelson Ijhi, Yaping Liu, Pratik Marolia, Henry Mitchel, Suchit Subhaschandra, Arthur Sheiman, Tim Whisonant, and Prabhhat Gupta. A reconfigurable computing system based on a cache-coherent fabric. In *2011 International Conference on Reconfigurable Computing and FPGAs*, pages 80–85, 2011.
- [37] Muhsen Owaida, Amit Kulkarni, and Gustavo Alonso. Distributed Inference over Decision Tree Ensembles on Clusters of FPGAs. *ACM Trans. Reconfigurable Technol. Syst.*, 12(4), September 2019.
- [38] Muhsen Owaida, David Sidler, Kaan Kara, and Gustavo Alonso. Centaur: A framework for hybrid CPU-FPGA databases. In *2017 IEEE 25th Annual International Symposium on Field-Programmable Custom Computing Machines (FCCM)*, pages 211–218. IEEE, 2017.
- [39] Parthasarathy Ranganathan, Daniel Stodolsky, Jeff Calow, Jeremy Dorfman, Marisabel Guevara, Clinton Wills Smullen IV, Aki Kuusela, Raghu Balasubramanian, Sandeep Bhatia, Prakash Chauhan, Anna Cheung, In Suk Chong, Niranjani Dasharathi, Jia Feng, Brian Fosco, Samuel Foss, Ben Gelb, Sara J. Gwin, Yoshiaki Hase, Da-ke He, C. Richard Ho, Roy W. Huffman Jr., Elisha Indupalli, Indira Jayaram, Poonacha Kongetira, Cho Mon Kyaw, Aaron Laursen, Yuan Li, Fong Lou, Kyle A. Lucke, JP Maaninen, Ramon Macias, Maire Mahony, David Alexander Munday, Srikanth Muroor, Narayana Penukonda, Eric Perkins-Argueta, Devin Persaud, Alex Ramirez, Ville-Mikko Rautio, Yolanda Ripley, Amir Salek, Sathish Sekar, Sergey N. Sokolov, Rob Springer, Don Stark, Mercedes Tan, Mark S. Wachler, Andrew C. Walton, David A. Wickeraad, Alvin Wijaya, and Hon Kwan Wu. Warehouse-Scale Video Acceleration: Co-Design and Deployment in the Wild. In *Proceedings of the 26th ACM International Conference on Architectural Support for Programming Languages and Operating Systems*, page 600–615, New York, NY, USA, 2021. Association for Computing Machinery.
- [40] C Ravishanar and James R Goodman. Cache implementation for multiple microprocessors. In *Proceedings of the 26th IEEE Computer Society International Conference (COMCON)*, 1983.
- [41] Mohammadsadegh Sadri, Christian Weis, Norbert Wehn, and Luca Benini. Energy and performance exploration of accelerator coherency port using xilinx zynq. In *Proceedings of the 10th FPGAWorld Conference*, pages 1–8, 2013.
- [42] David Sidler, Zsolt István, Muhsen Owaida, and Gustavo Alonso. Accelerating pattern matching queries in hybrid cpu-fpga architectures. In *Proceedings of the 2017 ACM International Conference on Management of Data*, pages 403–415, 2017.
- [43] David Sidler, Zsolt István, Muhsen Owaida, and Gustavo Alonso. Open sourced regular expression matching module, 2017.
- [44] John E Stone, David Gohara, and Guochun Shi. Opencl: A parallel programming standard for heterogeneous computing systems. *Computing in science & engineering*, 12(3):66, 2010.
- [45] J. Stuecheli, W. J. Starke, J. D. Irish, L. B. Arimilli, D. Dreps, B. Blaner, C. Wollbrink, and B. Allison. IBM POWER9 Opens up a New Era of Acceleration Enablement: OpenCAPI. *IBM J. Res. Dev.*, 62(4–5):8:1–8:8, July 2018.
- [46] Jeffrey Stuecheli, Bart Blaner, CR Johns, and MS Siegel. CAPI: A Coherent Accelerator Processor Interface. *IBM Journal of Research and Development*, 59(1):7:1–7:7, 2015.
- [47] C. K. Tang. Cache system design in the tightly coupled multiprocessor system. New York, NY, USA, 1976. Association for Computing Machinery.
- [48] The Wireshark Team. Wireshark. <https://www.wireshark.org>, 1998–2022.
- [49] Jan van Lunteren, Ronald Luijten, Dionysios Diamantopoulos, Florian Auernhammer, Christoph Hagleitner, Lorenzo Chelini, Stefano Corda, and Gagandeep Singh. Coherently attached programmable near-memory acceleration platform and its application to stencil processing. In *2019 Design, Automation & Test in Europe Conference & Exhibition (DATE)*, pages 668–673. IEEE, 2019.
- [50] Xilinx. Xilinx zynq ultrascale+ mp soc. <https://www.xilinx.com/products/silicon-devices/soc/zynq-ultrascale-mpsoc.html>, 2022.